

Received 4 April 2023, accepted 16 April 2023, date of publication 25 April 2023, date of current version 10 May 2023.

Digital Object Identifier 10.1109/ACCESS.2023.3270327

## RESEARCH ARTICLE

# Broadband Equivalent Modeling and Common-Mode Voltage Conduction Analysis of Electrochemical Energy Storage System

BO ZHAO<sup>1,2</sup>, JUAN HU<sup>1</sup>, DONG HUI<sup>1</sup>, ZHANZHAN QU<sup>1</sup>, LEI LIU<sup>2</sup>, AND CHAOFEI GAO<sup>1,2</sup>

<sup>1</sup>State Key Laboratory of Operation and Control of Renewable Energy and Storage Systems, China Electric Power Research Institute, Beijing 100192, China

<sup>2</sup>School of Automation, Beijing Information Science and Technology University, Beijing 100192, China

Corresponding author: Chaofei Gao (gaocf@bistu.edu.cn)

This work was supported by the Open Fund of Beijing Key Laboratory of Distribution Transformer Energy-Saving Technology (China Electric Power Research Institute) under Grant PDB51202001511.

**ABSTRACT** Electrochemical energy storage system play an important role in the reform of the national energy system and the construction of the energy Internet. Whether small or large capacity battery storage converters, the characteristics of their power electronics can generate high frequency common mode voltage that can be potentially harmful to battery storage system. This paper systematically investigates the common-mode interference (CMI) of electrochemical energy storage system. The mechanism of common-mode interference is revealed, a broadband equivalent circuit model of common-mode voltage in electrochemical energy storage system is established, the effect of parasitic capacitance of the battery on common-mode voltage is simulated and analyzed, and the broadband equivalent circuit model is verified based on laboratory data.


**INDEX TERMS** Electrochemical energy storage system, common mode voltage, broadband equivalent circuit.

## I. INTRODUCTION

As an important way of electrical energy storage, battery energy storage has the advantages that power and energy can be configured flexibly according to different application requirements, fast response time, not limited by external conditions such as geographical resources, suitable for large-scale applications and batch production, etc. Battery energy storage has an irreplaceable position in cooperation with centralized/distributed new energy grid-connected and grid operation assistance [1]. The battery energy storage system contains several components such as electrochemical batteries, power electronic converters, battery management system [2], and contactors, connection cables, etc. Whether it is a DC/DC+DC/AC two-stage converter for small-capacity battery storage or a DC/AC one-stage converter for medium-capacity and large-capacity battery storage, high-speed switching action of power devices in the

inverter can cause serious electromagnetic interference (EMI) problems [5].

Although the research and application of large-capacity energy storage is not long, common mode interference affecting the normal operation of the battery management system has been found at the site of large-capacity energy storage project in the southern power grid [6], and the common mode interference was measured at the DC-bus position, pointing out that the three-phase isolated transformer cannot completely solve the problem of common mode interference, but the generation and propagation path of common mode interference was not modeled and analyzed. In terms of the mechanism of common-mode interference generation Prof. Li Ying's team from North China Electric Power University proposes that there are potential connections and parasitic capacitive coupling between the energy supply system, the circuit breaker and the earth, and when overvoltage occurs in the circuit breaker and its bus, the corresponding transient electric field changes through the parasitic capacitive circuit to form common mode interference current, which generates common mode interference in the energy supply system [7].

The associate editor coordinating the review of this manuscript and approving it for publication was Diego Bellan .

L. Ran et al. from the University of Nottingham, studied the mechanism of conducted EMI radiation associated with a typical PWM inverter induction motor drive system [8]. Erkuan Zhong and Thomas A. Lipo from the University of Wisconsin, proposed that in motor drive system, the motor, the power switching device, and the longer feed line, may become the main noise source because of the large distributed capacitance [9].

Common mode voltage effects and research started from the field of switching power supplies [11], as early as 1983, corcom USA studied and described the common mode voltage characteristics and equivalent circuits of switching power supplies from the point of view of designing and producing power supply filters. E-System, USA, discussed the generation and modeling of EMI in switching power supplies and gave a method for fast prediction in frequency errors. In China, Prof. Yong Kang and Prof. The inverter contains switching power devices such as IGBTs, which generate high du/dt signals at the moment of switching action. The high du/dt signals generate common-mode currents through the distributed capacitance between the device and the protective ground, increasing the electromagnetic radiation of the system, so it is important to establish its prediction model for optimizing common-mode conducted EMI [13]. In order to better study the common-mode conduction of electrochemical energy storage system, the problem of common-mode interference associated with photovoltaic power generation was drawn upon. Foreign researchers at the Politecnico di Bari, Italy [14] developed a transformerless common-mode interference model with a detailed analysis of common-mode currents. Researchers at the University of Navarra, Spain, proposed a novel conversion topology for transformerless photovoltaic (PV) system that does not generate an alternating common-mode total voltage, thus improving the behavior of the inverter in terms of electromagnetic interference, exhibiting high efficiency, and not injecting DC into the grid [15]. Ruxiang Hao and Hong Li of Beijing Jiaotong University proposed an H5-D topology and its modulation strategy for transformerless PV inverters, which can effectively suppress the common mode current of PV inverters [16]. The team of Prof. Xing Zhang [17] from Hefei University of Technology addressed the common-mode current problem of non-isolated three-phase three-level PV inverter, and based on the analysis of the three-level common-mode equivalent model, an improved LCL filter was used to connect the common point of the filter capacitor back to the neutral point of the DC-side to filter out the high-frequency component of the parasitic capacitor voltage, resulting in a significant attenuation of the common-mode current. Wang Yi and Li He Ming et al. proposed that due to the technical characteristics of PWM modulation technology itself, it is decided that the inverter output AC power contains more higher harmonic components [18], and pointed out that the common mode voltage contains high-frequency harmonic components as the main reason for the common mode current.

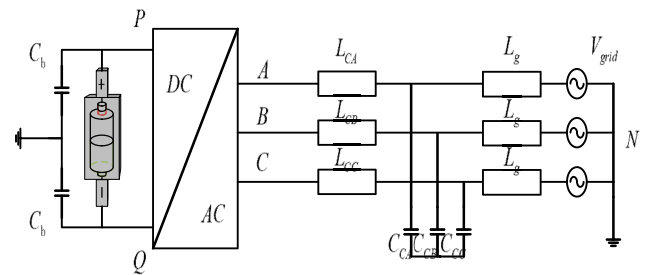


FIGURE 1. Non-isolated three-phase energy storage inverter structure.

Huafeng Xiao and Shaojun Xie from Nanjing University of Aeronautics and Astronautics, China [20] derived a high-frequency common-mode equivalent model for non-isolated single-phase inverters considering parasitic parameters and generalized two ways to eliminate common-mode currents based on this model. These research results have some implications for the study of this paper.

This paper investigates the problem of common mode voltage in electrochemical energy storage system. By studying and analyzing the causes of common-mode voltage generation in electrochemical energy storage system, a broadband equivalent circuit model of common-mode voltage in electrochemical energy storage system is established, the effects of common-mode conduction paths and cell-to-ground parasitic capacitance on common-mode conduction are analyzed, and field tests are carried out to verify the validity of the model.

## II. MECHANISM OF COMMON-MODE INTERFERENCE OF ELECTROCHEMICAL ENERGY STORAGE SYSTEM

### A. BASIC STRUCTURE OF NON-ISOLATED ELECTROCHEMICAL ENERGY STORAGE SYSTEM

The non-isolated battery energy storage system involves several components such as electrochemical batteries, power electronic converters, battery management system, and contactors, connection cables, etc. The electrochemical batteries provide a stable DC power supply for the energy storage system, and the DC power is converted to grid-specified AC power through the inverter. Its structure is shown in Fig. 1, where the parasitic parameter  $C_b$  is the parasitic capacitance of the energy storage battery to earth. The energy storage battery is measured with P terminal (DC+) and Q terminal (DC-), the potential is defined with reference to earth, the voltage fluctuation of P terminal and Q terminal will generate common mode current (leakage current) through the parasitic capacitance, the size of this leakage current depends on the magnitude frequency of the voltage and the size of the parasitic capacitance.  $L_{CA}$ ,  $L_{CB}$  and  $L_{CC}$  are the bridge arm filter inductors.  $L_g$  are the filter inductors on the network side.  $C_{CA}$ ,  $C_{CB}$  and  $C_{CC}$  are the filter capacitors. N is the neutral point of the grid connected to ground.

**B. CAUSE OF ALTERNATING VOLTAGE BETWEEN DC-BUS AND GROUND**

In the non-isolated three-phase PV inverter structure, the solar panel and the grid are electrically connected, which makes the common-mode current increase significantly and brings conducted and radiated disturbances. For the non-isolated three-phase energy storage inverter system, there is also a potential connection between the energy storage battery and the grid neutral, and when the system is operating normally, common mode interference is generated by the inverter system through the grid neutral and the storage battery parasitic capacitance to form common mode currents  $I_{cm}$ . As shown in Fig. 2.

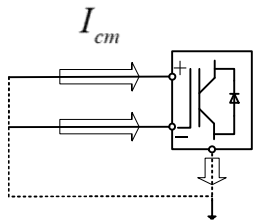


**FIGURE 2. Common mode current loop.**

In the grid connection process of battery energy storage system, the DC voltage needs to be pulse modulated to meet the grid connection requirements, so the DC power supply is alternately connected to the semiconductor switches, and through the high frequency conduction and shutdown of the switch tube, the voltage from the DC-side to the reference center or to the earth generates oscillations in the form of a square wave-like [21]. Energy storage terminals are labeled as P (DC+terminal) and Q (DC-terminal), Their potential is relative to the ground. Assuming that the neutral point on the DC-side is point N\*, the neutral point of the grid is point N, and for a grounded system point N is connected to the location, then the phase voltage can be defined as:

$$\begin{cases} u_{NA} = u_{N^*A} - u_{N^*N} \\ u_{NB} = u_{N^*B} - u_{N^*N} \\ u_{NC} = u_{N^*C} - u_{N^*N} \end{cases} \quad (1)$$

Assume that the load circuit is three-phase symmetric, the sum of  $u_{NA}$ ,  $u_{NB}$  and  $u_{NC}$  is zero, therefore, by organizing equation (1), the voltage between N\* and N can be obtained as follows:

$$u_{N^*N} = \frac{1}{3}(u_{N^*A} + u_{N^*B} + u_{N^*C}) \quad (2)$$

According to equation (2), it can be deduced that there are four values of  $u_{N^*N}$ ,  $\pm u_{DC}/2$  and  $\pm u_{DC}/6$ , respectively. Therefore, the voltage expressions of energy storage terminals P (DC+ terminal) and Q (DC- terminals) to ground are:

$$\begin{cases} u_{PN} = +\frac{u_{DC}}{2} + u_{N^*N} \\ u_{QN} = -\frac{u_{DC}}{2} + u_{N^*N} \end{cases} \quad (3)$$

Due to the characteristics of the inverter itself will make the DC-side of the grid-connected energy storage system to

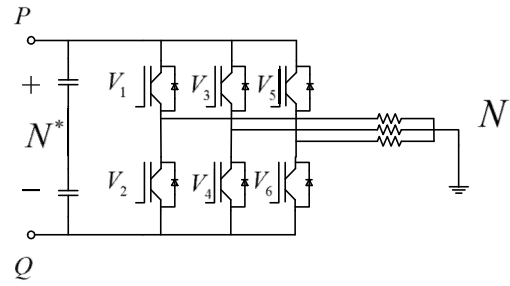


**FIGURE 3. Three-phase bridge inverter topology.**

ground voltage oscillation, that is, the source of common-mode interference, and due to the existence of parasitic capacitance of electrochemical cells to ground, will generate common-mode current and thus affect the stable operation of the battery management system, but also affect the battery insulation material, and in serious cases may lead to system failure.

**III. COMMON-MODE EQUIVALENT MODEL AND CALCULATION ANALYSIS OF THREE-PHASE INVERTER**

In this section, the common-mode equivalent circuits of non-isolated and isolated three-phase energy storage inverters are modeled, and the effects of parasitic parameters on common-mode voltage and the causes of common-mode interference suppression in isolated three-phase inverter system are calculated and analyzed.

**A. COMMON-MODE EQUIVALENT MODEL OF INVERTER OF NON-ISOLATED THREE-PHASE ENERGY STORAGE SYSTEM**

Voltage fluctuations at the P and Q terminals cause leakage current to flow to ground through the parasitic capacitance of the energy storage cell to ground, however, the level of common mode voltage depends on the amplitude and frequency of the leakage current fluctuations and the value of the parasitic capacitance. Fig. 4 establishes the common-mode equivalent model of the inverter of the three-phase energy storage system; the presence of the parasitic capacitance of the energy storage battery to ground makes the DC-bus connected to the grid-side neutral ground, which in turn provides a circuit for common-mode interference. In Fig. 4,  $V_{PA}$ ,  $V_{PB}$  and  $V_{PC}$  are the common-mode interference sources in each phase, respectively; the bridge arm filter inductors  $L_{CA}$ ,  $L_{CB}$  and  $L_{CC}$ ; the filter inductors  $L_g$  on the net side; the net-side filter capacitors  $C_{CA}$ ,  $C_{CB}$  and  $C_{CC}$ ; the parasitic capacitance  $C_C$ , generated by the filter; and the inductance  $L_{cg}$  between the DC-side and ground;  $C_B$  is the energy storage battery parasitic capacitance and  $C_B=2 \times C_b$ .

Through the above analysis the expression for common mode interference can be defined as:

$$V_{CM3} = \frac{V_{PA} + V_{PB} + V_{PC}}{3} \quad (4)$$

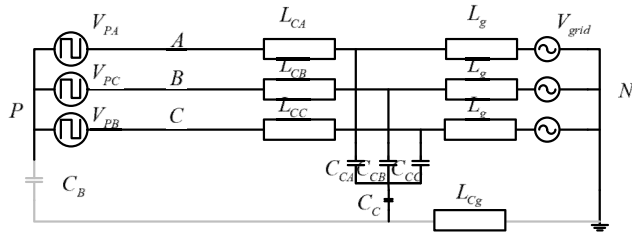


FIGURE 4. Common mode equivalent model of three-phase energy storage inverter system.

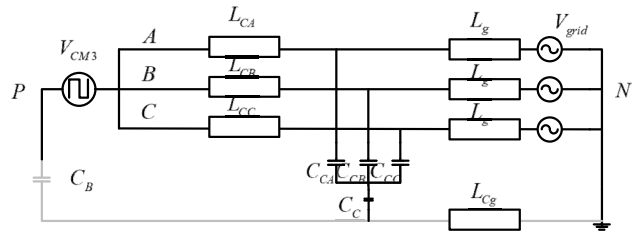


FIGURE 5. Schematic diagram of common mode equivalent model of three-phase energy storage inverter system.

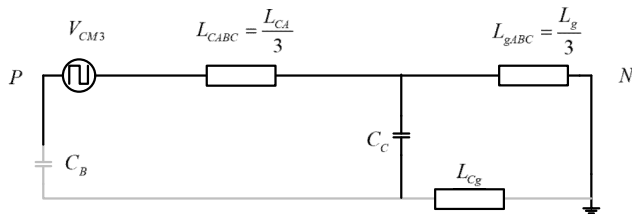


FIGURE 6. Schematic diagram of common mode equivalent model of three-phase energy storage inverter system.

The model based on the above equation can be simplified as shown in Fig. 5.

As can be seen from Fig. 5, the filter inductor of each phase bridge arm and the filter inductor of the net side are connected in parallel, for the filter parasitic capacitance has a large capacitive resistance compared to the filter capacitor, then the filter parasitic capacitance will play a dominant role, and the simplified common-mode equivalent model of the three-phase inverter is shown in Fig. 6.

By drawing on the impedance model of the PV grid-connected inverter system [22], a common-mode equivalent model common-mode loop impedance model of the non-isolated energy storage inverter system was developed, as shown in Fig. 7.

The common mode voltage equation for the parasitic capacitance of the energy storage cell is shown in equation (5):

$$V_{CM-CB} = V_{CM3} \times \frac{Z_{CB}}{\frac{Z_g \times Z_{Cg}}{Z_g + Z_{Cg}} + 1 + Z_{CB} + Z_{CABC}} \quad (5)$$

$V_{CM-CB}$  indicates the common mode voltage of the energy storage system. Considering the influence of the parasitic

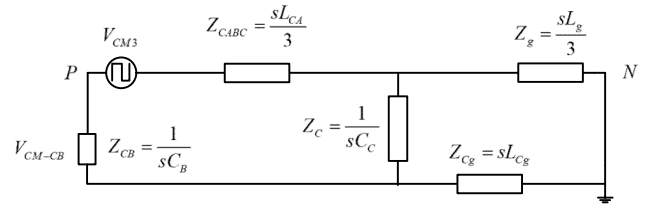


FIGURE 7. Common mode impedance model of non-isolated energy storage inverter system.

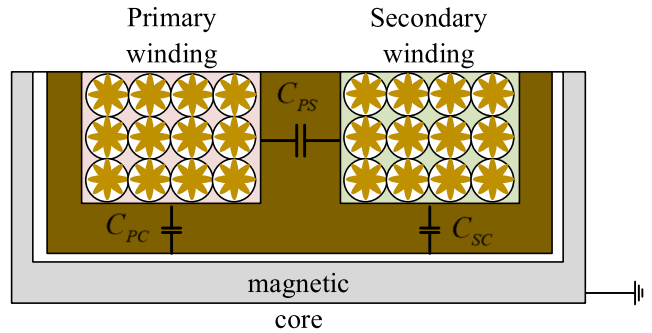


FIGURE 8. Schematic diagram of distributed capacitance structure of high frequency transformer.

capacitance  $C_C$  generated by the filter on  $V_{CM-CB}$ , the analysis of equation (5) shows that the capacitance of  $C_C$  shows a positive correlation with  $V_{CM-CB}$ , and the analysis of equation (6) shows that the capacitance of  $C_B$  shows a negative correlation with  $V_{CM-CB}$ .

$$V_{CM-CB} = V_{CM3} \times \frac{1}{\frac{Z \times Z_C + Z_{CABC}}{Z + Z_C} + 1 + Z_{CB}} \quad (6)$$

## B. COMMON-MODE EQUIVALENT MODEL OF TRANSFORMER-ISOLATED THREE-PHASE ENERGY STORAGE GRID-CONNECTED INVERTER SYSTEM

High-frequency transformers are essential as key components for electrical isolation as well as electrical energy conversion, and the reduced size of high-frequency transformers and compact design of windings structures lead to a significant increase in the influence of transformer stray parameters, especially the distributed capacitance, which affects the performance of the converter [23]. For energy storage grid-connected system, it is crucial to analyze the distributed capacitance of the transformer. A common-mode equivalent model of a three-phase energy storage grid-connected inverter with transformer is developed through Fig. 5.

The schematic diagram of the distributed capacitance structure of the high-frequency transformer is shown in Fig. 8. High frequency transformer is divided into three parts, which are primary windings, secondary windings and magnetic core. Its distributed capacitance includes capacitance  $C_{PS}$  between primary and secondary windings, capacitance  $C_{PC}$  between primary windings and core, capacitance  $C_{SC}$  between secondary windings and core, and generally

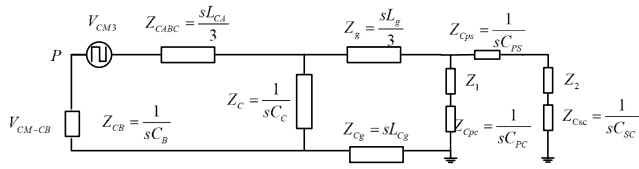


FIGURE 9. Common-mode equivalent impedance model of three-phase energy storage grid-connected inverter system with transformer.

the core is required to be grounded at a single point. The common-mode equivalent model of the three-phase energy storage grid-connected inverter system with transformer is constructed according to Fig. 8 and shown in Fig. 9.

$Z_1$  denotes the primary windings impedance magnitude and  $Z_2$  denotes the secondary windings impedance magnitude. Since the capacitance  $C_{PS}$  between the primary and secondary windings and the capacitance  $C_{SC}$  between the secondary windings and the core are very small values, without considering the common mode interference conduction to the network side, only analyze what effect the energy storage system will have on the common mode loop of the inverter side by adding an isolation transformer, and derive the common mode voltage formula of the parasitic capacitance of the energy storage battery according to Fig. 10 in equation (7).

$$V_{CM-CB} = \frac{V_{CM3} \times Z_{CB}}{\frac{Z_C}{1 + \frac{Z_g + Z_{Cg} + Z_1 + Z_{Cps}}{Z_C}} + Z_{CB} + Z_{CABC}} \quad (7)$$

The value of  $V_{CM-CB}$  is particularly small according to equation (7), which can be understood as the primary windings of the isolation transformer is not grounded, blocking the common mode circuit of the inverter and thus achieving the purpose of common mode interference suppression. The above is only a qualitative analysis of the common-mode voltage, which matches the laboratory simulation results; for the quantitative analysis, it is difficult to obtain the mathematical expression of the common-mode voltage source or the expression is very complicated, so the amplitude and frequency of the common-mode voltage cannot be calculated.

#### IV. SIMULATION ANALYSIS OF COMMON-MODE VOLTAGE BASED ON BROADBAND EQUIVALENT MODEL

This section carries out the simulation analysis of the common-mode conduction of the three-phase voltage-based bridge inverter circuit, considering only the case of the parasitic capacitance of the energy storage battery, and the main parameters of the experimental non-isolated energy storage inverter system are shown in table 1.

##### A. INTRODUCTION OF PARASITIC PARAMETERS

The parasitic capacitance distribution parameters of the energy storage cells to ground are related to the arrangement topology of the cells in the pack, where each single cell housing is connected to the case, which is electrically connected to ground, the parasitic parameters introduced by the battery

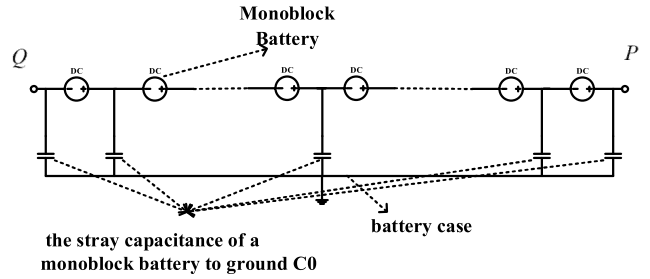


FIGURE 10. Equivalent diagram of battery system stray capacitance.

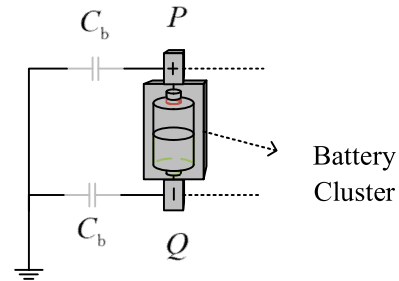


FIGURE 11. Schematic diagram of the positive and negative poles of the battery system to the ground capacitance respectively.

pack mainly include stray capacitance between the individual cells (front and side), and the equivalent capacitance of the single cell to the case, since it is difficult to obtain the exact value of the parasitic elements, the typical value of the equivalent capacitance of the battery monomer to the case is obtained by measurement as 0.4 nF, the parasitic capacitance between the battery singles can be neglected. The battery system stray capacitance equivalence diagram is shown in Fig. 10. Based on the principle of equal total leakage current, the stray capacitance of a monoblock battery to ground is equated to the capacitance of the positive and negative terminals of the system to ground, as shown in Fig. 11.

Based on the principle of equal total leakage current, the stray capacitance of the battery cluster to ground is equal to the capacitance of the positive and negative terminals of the system to ground in equation (8), therefore, equation (9) can be derived.

$$I_{CMtotal} = \sum I_{CMsingle} \quad (8)$$

$$\sum_{i=1}^n C_0 \frac{du_i}{dt} = C_0 \sum_{i=1}^n \frac{d \frac{(n-1)u_- + iu_+}{n}}{dt} \quad (9)$$

The value of the parasitic capacitance of the government bus to ground can be deduced from Equation (9) in equation (10).

$$\frac{n}{2} C_0 \frac{du_-}{dt} + \frac{n}{2} C_0 \frac{du_+}{dt} \Rightarrow \begin{cases} C_+ = \frac{n}{2} C_0 \\ C_- = \frac{n}{2} C_0 \end{cases} \quad (10)$$

The voltage of a certain model of single battery is 3V, and this paper mentions that the DC voltage should reach

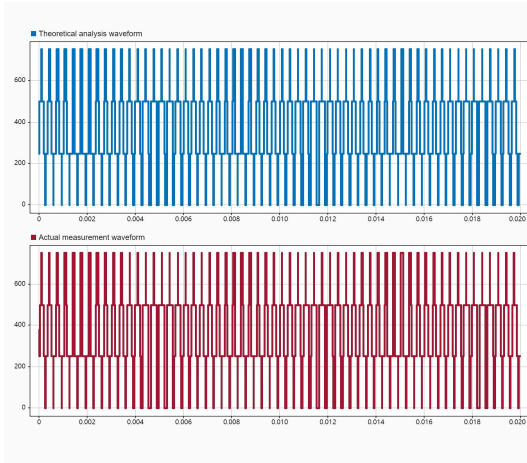


**FIGURE 12. Positive DC-bus to ground voltage waveform verification diagram.**

750V, so 250 single batteries are needed. And a battery box has 10 battery monomer composition, showing two rows of arrangement, so 25 battery boxes are needed. In which, each single battery case is connected to the box, and the box is electrically connected to the earth, according to equation (10) can be deduced from the positive and negative busbar to ground equivalent capacitance is  $C_b = 0.4 \times (250/2) \times 10^{-9}$  F. Then the value of the parasitic capacitance of the broadband equivalent model in this paper is  $C_B = 2 \times C_b = 0.4 \times 250 \times 10^{-9}$  F.

**B. BROADBAND EQUIVALENT MODEL SIMULATION EXPERIMENT**

The experimental simulation in this section confirms the principle described in the summary of 1.2. Due to the nature of the inverter itself, the DC-side voltage will be connected to the reference ground through the power switching tubes, making it generate a square wave-like oscillation waveform, which will affect the subsequent currents through the parasitic capacitance of the energy storage battery to ground to generate stronger common mode interference as well as through the parasitic capacitance to generate leakage current and common mode current through ground to affect the subsequent circuits. The positive DC-bus to ground voltage waveform is shown in Fig. 12.

The broadband equivalent model of the non-isolated three-phase energy storage inverter system is inputted into MATLAB/SIMULINK. The interference source of the common-mode equivalent model is generated by combining the two-level inverter topology with bipolar control, setting three modulation signals with phase difference of  $2\pi/3$  and 50 Hz in turn, and the carrier signal is set to 4.8 kHz bipolar triangle wave with a modulation system of 0.95. In order to derive the effect of the parasitic capacitance of the energy storage cell to ground on the common mode voltage waveform amplitude and frequency, a comparison was done

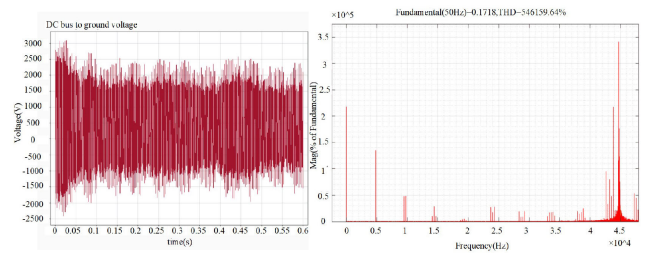


**FIGURE 13. Common mode voltage waveform and spectrum diagram under working condition 1.**

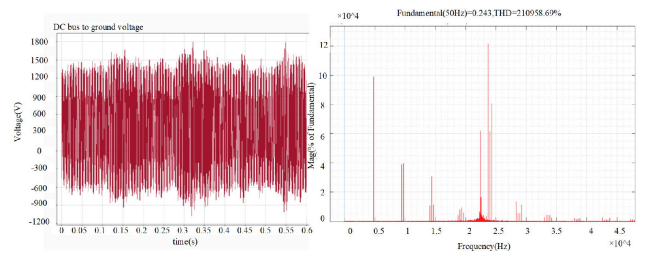


**FIGURE 14. Common mode voltage waveform and spectrum diagram under working conditions 2.**

for three working conditions, taking  $C_B/4$ ,  $C_B$  and  $2 \times C_B$  respectively for the test.

**1) WORKING CONDITION 1**

The main parameters are shown in Table 1 and taken as  $C_B^* = C_B/4 = 0.1 \times 250 \times 10^{-9}$  F. Under this condition, the positive DC-bus voltage waveform obtained from the simulation and its spectrum is shown in Fig. 13, it can be seen from the spectrum that its frequency is mainly the switching frequency  $f_c$  and the 7th harmonic etc. and its vicinity, and its amplitude range is  $-1500$  V -  $+2500$  V.

**2) WORKING CONDITION 2**

The main parameters are shown in Table 1 and taken as  $C_B^* = C_B = 0.4 \times 250 \times 10^{-9}$  F. Under this condition, the positive DC-bus voltage waveform obtained from the simulation and its spectrum is shown in Fig. 14, it can be seen from the spectrum that its frequency is mainly the switching frequency  $f_c$  and the 5th harmonic etc. and its vicinity, and its amplitude range is  $-900$  V -  $+1600$  V.

**3) WORKING CONDITION 3**

The main parameters are shown in Table 1 and taken as  $C_B^* = 2 \times C_B = 0.8 \times 250 \times 10^{-9}$  F. Under this condition, the positive DC-bus voltage waveform obtained from the simulation and its spectrum is shown in Fig. 15, it can be seen from the spectrum that its frequency is mainly the switching frequency  $f_c$  and the 3th harmonic etc. and its vicinity, and its amplitude range is  $-800$  V -  $+1400$  V.

Through the simulation experiments of three working conditions, the information of the parasitic capacitance taking

**TABLE 1.** Main parameter table of non-isolated energy storage inverter system.

Parameter	Value	Parameter	Value
DC voltage	750V	Filter inductor	4.1mH
Grid voltage	380V	Filter capacitor	120μF
Power frequency	50Hz	Parasitic capacitance	100nF

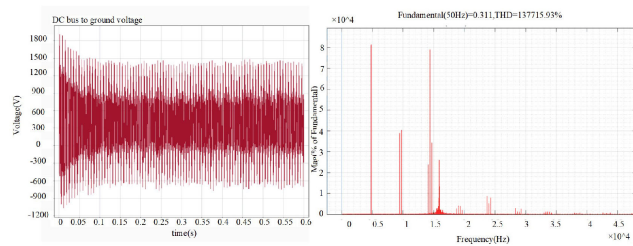


**FIGURE 15.** Common mode voltage waveform and spectrum diagram under working conditions 3.

**TABLE 2.** Amplitude and frequency comparison table of DC-bus to ground voltage waveform in three working conditions.

Parameter	Statistical time/min for each level		
	Condition 1	Condition 2	Condition 3
Parasitic capacitance	0.1 nF	0.4 nF	0.8 nF
Amplitude	- 1500 V - + 2500 V	- 900 V - + 1600 V	- 800 V - + 1400 V
Frequency	≈ 45 kHz	≈ 24 kHz	≈ 15 kHz

values of 0.1 nF, 0.4 nF and 0.8 nF, respectively, is organized in table 2.

According to Table 2, the larger the parasitic capacitance, the smaller the common mode voltage waveform amplitude, and vice versa; the larger the parasitic capacitance, the lower the common mode voltage waveform frequency. Comparing with equation (6), when the parasitic capacitance is small, the oscillation frequency is large, which reflects the common mode interference becomes stronger; when the parasitic capacitance is large, the oscillation frequency is small, which reflects the common mode interference becomes weaker.

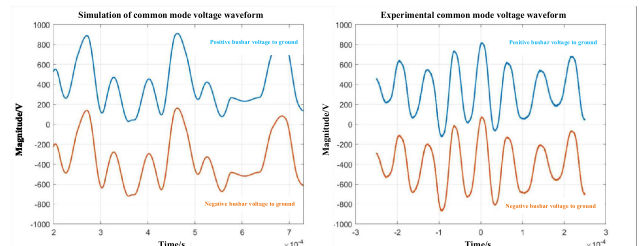


**FIGURE 16.** Comparison of common mode voltage between experimental test and model simulation.

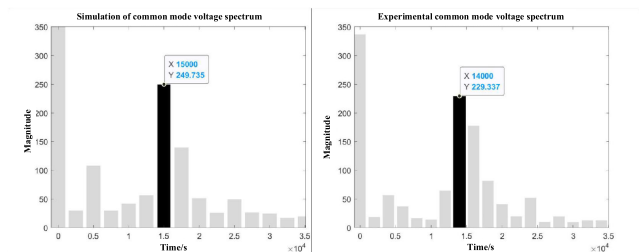


**FIGURE 17.** Comparison of common mode voltage spectrum between experimental test and model simulation.

**V. LABORATORY TESTING OF COMMON-MODE VOLTAGE OF ELECTROCHEMICAL ENERGY STORAGE SYSTEM**

The basic structure of the circuit is shown in Fig. 1, and the parameters of the experimental system are shown in table 1. The PCS system is measured in standby to charging operation, and the monitored voltage locations are positive DC-bus to ground and negative DC-bus to ground.

Fig. 16 shows the common-mode voltage waveforms of the experimental test and the simulated waveforms of the broadband equivalent model. Fig. 17 shows the common-mode voltage spectrogram of the experimental test and the common-mode voltage spectrogram of the broadband equivalent model. The voltage value of the DC-side power supply positive to the case of the PCS was tested, the monitoring voltage starts to oscillate when the system changes from standby to charging operation, and the monitoring voltage waveforms corresponding to the positive and negative busbar are the same. Due to the switching frequency of the system is 4.8 kHz as well as the oscilloscope storage capacity limit, the manufacturer only provides the data of field 0.5 ms, so the analysis

of the low frequency band spectrum is not accurate, this paper mainly compares and analyzes the high frequency band of the experimental test and model simulation spectrogram. From the experimental test waveform, it can be seen that the voltage amplitude range is  $-124\text{ V} - +812\text{ V}$  and the frequency is mainly distributed around  $14\text{ kHz}$ , which is equivalent to about  $\pm 500\text{ V}/14\text{ kHz}$  AC superimposed on the DC power supply of standby  $\pm 350\text{ V}$ , the broadband equivalent model simulation results show a voltage amplitude range of  $+20\text{ V} - +887\text{ V}$  and the frequency is mainly distributed around  $15\text{ kHz}$ , which is equivalent to about  $\pm 500\text{ V} / 15\text{ kHz}$  AC superimposed on the DC power supply of standby  $\pm 350\text{ V}$ . It can be seen that the common mode voltage amplitude and frequency of the experimental test and model simulation are basically the same, which verifies the validity of the common mode voltage equivalent model proposed in this paper, but the error in the measurement of the parasitic capacitance of the energy storage battery to ground will cause the difference of the oscillation frequency.

From Fig. 16 and Fig. 17, it can be seen that there are still differences between the common mode voltage waveforms simulated using the broadband equivalent model and the laboratory test waveforms provided by the manufacturer, and there are also differences in the amplitude and frequency of the oscillation modes in other high frequency bands. This is because the broadband equivalent model proposed in this paper only considers the effect of the parasitic capacitance of the energy storage battery on the ground, but not the parasitic capacitance parameters of other modules such as DC cable, AC cable, converter module, etc. This needs to be improved in the next work to gradually improve the accuracy of the broadband equivalent model of the electrochemical energy storage system.

## VI. CONCLUSION

This paper systematically investigates the common-mode interference (CMI) of electrochemical energy storage systems. The mechanism of common-mode interference is revealed, a broadband equivalent circuit model of common-mode voltage of electrochemical energy storage system is established, the effect of parasitic capacitance of the battery on common-mode voltage is simulated and analyzed, and the broadband equivalent circuit model is verified based on laboratory data, the main conclusions are as follows:

For a non-isolated three-phase energy storage inverter system, there is an electrical connection between the energy storage battery and the grid neutral. When the system is operating normally, common mode interference is generated by the inverter system through the grid neutral and the parasitic capacitance of the energy storage battery to form a common mode current loop.

Based on the broadband equivalent circuit model of the three-phase energy storage inverter system, the relationship between the magnitude of the parasitic capacitance of the battery to ground and the amplitude of the common-mode interference voltage is analyzed. For the isolated three-phase

energy storage inverter system, because the distributed capacitance between the primary windings and the magnetic cores is exceptionally small leading to its exceptionally high capacitive reactance, blocking the inverter common-mode loop, thus achieving the purpose of suppressing common-mode interference.

Based on the laboratory test waveform of a manufacturer, the broadband equivalent model in this paper was compared and verified, and the experimental results shows that the analysis results of the equivalent model mentioned in this paper were basically consistent with the laboratory test waveform.

The next work should mainly focus on 1) improving the accuracy of the measurement of the parasitic capacitance of the energy storage cell to the ground; 2) carrying out the analysis of the influence of the distributed capacitance of other modules of the electrochemical energy storage system on the common mode voltage distribution, further improving the broadband equivalent model, and further improving the accuracy of the broadband equivalent model of this electrochemical energy storage system through the above work.

## REFERENCES

- [1] X. Li, S. Wang, and D. Hui, "Summary and prospect of operation control and application method for battery energy storage system," *Power Syst. Technol.*, vol. 41, no. 10, pp. 3315–3325, 2017.
- [2] J. Li, Y. Wu, N. Wang, J. Xiong, and S. Ma, "Review of information architecture and security system of Gigawatt electrochemical energy storage power station," *Automat. Electr. Power Syst.*, vol. 45, no. 23, pp. 179–191, 2021.
- [3] Y. Gao, X. Chen, Y.-F. Shi, J.-X. Zhu, and X.-F. Zhang, "Design and research on temperature acquisition circuit for battery management system," *Power Technol.*, vol. 42, no. 12, pp. 1901–1903, 2018.
- [4] H. Ni, X. Chen, J. Zhu, S. Lü, and A. Chu, "Design and research on voltage sampling circuit of battery management system," *Mod. Electron. Technique*, vol. 40, no. 10, pp. 158–160, 2017.
- [5] Z. Tianxiang, C. Henglin, Y. Wenqi, and S. Guobin, "Terminal common-mode electromagnetic interference modeling of inverter based on high-pass filter measurement," *Proc. CSEE*, vol. 42, no. 13, pp. 1–10, Jan. 2022.
- [6] B. Liu, Y. Li, C. Zhong, and G. Pan, "Analysis and research of common mode interference problem of large capacity battery energy storage system," *Mech. Elect. Technique Hydropower Station*, vol. 38, no. S1, pp. 85–88, 2015.
- [7] L. Ying, C. Xiang, and Z. Sheng, "Generation mechanism and suppression measure of common-differential mode interference in energy supply system of hybrid DC breaker," *Proc. CSEE*, vol. 40, no. 5, pp. 1722–1730, 2020.
- [8] L. Ran, S. Gokani, J. Clare, K. J. Bradley, and C. Christopoulos, "Conducted electromagnetic emissions in induction motor drive systems. I. Time domain analysis and identification of dominant modes," *IEEE Trans. Power Electron.*, vol. 13, no. 4, pp. 757–767, Jul. 1998, doi: 10.1109/63.704152.
- [9] L. Ran, S. Gokani, J. Clare, K. J. Bradley, and C. Christopoulos, "Conducted electromagnetic emissions in induction motor drive systems. II. Frequency domain models," *IEEE Trans. Power Electron.*, vol. 13, no. 4, pp. 768–776, Jul. 1998, doi: 10.1109/63.704154.
- [10] E. Zhong and T. A. Lipo, "Improvements in EMC performance of inverter-fed motor drives," *IEEE Trans. Ind. Appl.*, vol. 31, no. 6, pp. 1247–1256, Nov./Dec. 1995.
- [11] M. Nave, "Prediction of conducted emissions in switch mode power supplies," in *Proc. IEEE Int. Symp. EMC*, San Diego, CA, USA, Sep. 1986, pp. 167–173.
- [12] W. Teulings, J. L. Schanen, and J. Roudet, "A new technique for spectral analysis of conducted noise of a SMPS including interconnects," in *Proc. Rec. 28th Annu. IEEE Power Electron. Spec. Conf., Power Conditioning Spec. Conf., Power Process. Electron. Spec. Conf.*, Jun. 1997, pp. 1516–1521.



[13] P. Xinping, L. Hui, L. Li, and Y. Yisheng, "EMI prediction and analysis of common mode conducted interference of locomotive auxiliary inverter," in *High Voltage Apparatus*. Xi'an, China, 2022.

[14] L. M. Schneider, "Noise source equivalent circuit model for off-line converters and its use in input filter design," in *Proc. IEEE Int. Symp. Electromagn. Compat.*, Arlington, VA, USA, Aug. 1983, pp. 1–9, doi: [10.1109/IEMC.1983.7567390](https://doi.org/10.1109/IEMC.1983.7567390).

[15] L. N. de Souza, R. A. M. Braga, and F. B. Libano, "Introduction to conducted electromagnetic emission from inverted-fed induction motor drives according to the electromagnetic compatibility (EMC) requirements," in *Proc. IEEE Russia Power Tech*, Jun. 2005, pp. 1–6, doi: [10.1109/PTC.2005.4524691](https://doi.org/10.1109/PTC.2005.4524691).

[16] H. Li, C. Fang, R. Hao, T. Shao, and W. Su, "Research on the mechanism of harmonic generation and suppressing methods for photovoltaic grid-connected inverter with active clamp circuit," *Proc. CSEE*, vol. 37, no. 23, pp. 6971–6980, 2017.

[17] X. Zhang, Z. Shao, F. Wang, and P. Liu, "Leakage current reduction for transformerless three-phase three-level photovoltaic inverters," *Proc. CSEE*, vol. 33, no. 3, pp. 29–36, 2013.

[18] Y. Wang, H.-M. Li, X.-C. Shi, and L. Zhu, "Harmonic analysis and output filter design for multilevel PWM inverters," *Proc. CSEE*, vol. 10, pp. 78–82, Jan. 2003.

[19] T. Kerekes, R. Teodorescu, and M. Liserre, "Common mode voltage in case of transformerless PV inverters connected to the grid," in *Proc. IEEE Int. Symp. Ind. Electron.*, Jun. 2008, pp. 2390–2395.

[20] H.-F. Xiao, S.-J. Xie, W. Chen, and L. Gong, "Study on leakage current model for transformerless photovoltaic grid-connected inverter," *Proc. CSEE*, vol. 30, no. 18, pp. 9–14, 2010.

[21] S. Mercier and P. Boos, "Common mode management in BESS," SOCOMEC, Brookfield, WI, USA, Tech. Rep., Mar. 2020.

[22] Z. Chang, X. Zhang, F. Liu, F. Li, H. Xu, and R. Cao, "Common mode resonance characteristic research on paralleled three-level PV string inverters system," *Acta Energetica Solaris Sinica*, vol. 38, no. 9, pp. 2394–2402, 2017.

[23] W. Zhao, M. Zheng, and Q. Jiang, "Calculation method for parasitic capacitance of high frequency transformers," *J. Tsinghua Univ., Natural Sci. Ed.*, vol. 61, no. 10, pp. 1088–1096, 2021.



**BO ZHAO** was born in Qingdao, China, in 1977. He received the B.S. and M.S. degrees in electrical engineering from the Beijing University of Aeronautics and Astronautics, in 2000 and 2003, respectively, and the Ph.D. degree in electrical engineering from the China Electric Power Research Institute, in 2013. He was an Electrical Engineer with the China Electric Power Research Institute, State Grid of China. Since 2018, he has been with the Beijing Information Science and

Technology University, where he is currently a Researcher/professor-level Senior Engineer. His current research interests include the analysis and control of new energy and energy storage and the protection and control of microgrid.



**JUAN HU** was born in Hubei, China, in 1978. She received the B.S. and M.S. degrees from Hunan University, in 2000 and 2003, respectively. Since 2003, she has been with the China Electric Power Research Institute, where she is currently a Senior Engineer. Her current research interests include energy storage, power electronics, and flexible ac transmission.



**DONG HUI** was born in Henan, China, in 1968. He received the professor-level Senior Engineer, the Chief Technical Expert of the China Electric Power Research Institute, the Chairperson of the National Technical Committee of Electric Power Energy Storage Standardization, and the Secretary-General of the Professional Committee of Electric Power Energy Storage of China Electrical Engineering Society. His current research interests include large-scale energy storage technology, new energy and distributed power generation, and power electronics.



**ZHANZHAN QU** was born in Jiangsu, China, in 1986. He received the M.E. degree in electrical engineering from the School of Electrical and Electronic Engineering, North China Electric Power University, in 2012. His current research interests include electrical energy conversion and storage technology.



**LEI LIU** was born in Lanzhou, China, in 1998. He received the B.Eng. degree from the School of Automation, Beijing Information Science and Technology University, Beijing, China, in 2020, where he is currently pursuing the master's degree. His current research interests include new energy generation and grid frequency regulation.



**CHAOFEI GAO** was born in Shijiazhuang, China, in 1986. He received the B.S., M.S., and Ph.D. degrees in electrical engineering from North China Electric Power University, in 2008, 2011, and 2019, respectively. He was an Electrical Engineer with Shandong Power Supply Company, State Grid of China, from 2011 to 2015. He was a Visiting Scholar with the Center for Power Electronics Systems, Virginia Tech, from 2018 to 2019. He is currently an Associate Professor with the Beijing Information Science and Technology University. His current research interest includes the condition monitoring of power apparatuses.

...